

Comparative Analysis of Floc Measurement Setups for Characterising Settling Velocities and Size Distributions

Ali, Waqas; Kirichek, Alex ; Manning, Andrew J.; Chassagne, Claire

DOI

[10.3390/jmse13020212](https://doi.org/10.3390/jmse13020212)

Publication date

2025

Document Version

Final published version

Published in

Journal of Marine Science and Engineering

Citation (APA)

Ali, W., Kirichek, A., Manning, A. J., & Chassagne, C. (2025). Comparative Analysis of Floc Measurement Setups for Characterising Settling Velocities and Size Distributions. *Journal of Marine Science and Engineering*, 13(2), Article 212. <https://doi.org/10.3390/jmse13020212>

Important note

To cite this publication, please use the final published version (if applicable). Please check the document version above.

Copyright

Other than for strictly personal use, it is not permitted to download, forward or distribute the text or part of it, without the consent of the author(s) and/or copyright holder(s), unless the work is under an open content license such as Creative Commons.

Takedown policy

Please contact us and provide details if you believe this document breaches copyrights. We will remove access to the work immediately and investigate your claim.

Article

Comparative Analysis of Floc Measurement Setups for Characterising Settling Velocities and Size Distributions

Waqas Ali ^{1,*}, Alex Kirichek ² , Andrew J. Manning ^{3,4} and Claire Chassagne ^{1,*}

¹ Section of Environmental Fluid Mechanics, Department of Hydraulic Engineering, Faculty of Civil Engineering and Geosciences, Delft University of Technology, Stevinweg 1, 2628 CN Delft, The Netherlands

² Section of Rivers, Ports, Waterways and Dredging Engineering, Department of Hydraulic Engineering, Faculty of Civil Engineering and Geosciences, Delft University of Technology, Stevinweg 1, 2628 CN Delft, The Netherlands; o.kirichek@tudelft.nl

³ School of Biological and Marine Sciences, University of Plymouth, Plymouth PL4 8AA, UK; a.manning@plymouth.ac.uk

⁴ Coasts and Oceans Group, HR Wallingford, Wallingford OX10 8BA, UK

* Correspondence: w.ali@tudelft.nl (W.A.); c.chassagne@tudelft.nl (C.C.)

Abstract: Floc size distribution and settling velocities are crucial parameters for characterising cohesive sediments, as they influence how these sediments behave in various environmental settings. The accurate measurement of these properties is essential, with different methods available depending on the scope of the study. For long-term monitoring, in situ techniques based on laser diffraction are commonly used, while video microscopy techniques are preferred for shorter studies due to their ability to provide detailed information on individual particles. This study compares two high-magnification digital video camera setups, LabSFLOC-2 and FLOCCAM, to investigate the impact of particle concentration on settling velocity in flocculated sediments. Flocculated clay was introduced into settling columns, where both the size and settling velocities of the flocs were measured. The results obtained from both setups are in line with each other, even though the FLOCCAM was slightly more efficient at capturing images of small particles (of size less than 50 microns) and LabsFLOC-2 was better at detecting large size fraction particles (having a low contrast due to the presence of organic matter). Floc size and settling velocity measurements from both setups however exhibit mostly similar trends as a function of clay concentration and the same order of magnitudes for the recorded settling velocities.

Keywords: flocculation; settling velocities; particle size; cohesive sediment



Academic Editor: Markes E. Johnson

Received: 8 December 2024

Revised: 13 January 2025

Accepted: 21 January 2025

Published: 23 January 2025

Citation: Ali, W.; Kirichek, A.; Manning, A.J.; Chassagne, C. Comparative Analysis of Floc Measurement Setups for Characterising Settling Velocities and Size Distributions. *J. Mar. Sci. Eng.* **2025**, *13*, 212. <https://doi.org/10.3390/jmse13020212>

Copyright: © 2025 by the authors. Licensee MDPI, Basel, Switzerland. This article is an open access article distributed under the terms and conditions of the Creative Commons Attribution (CC BY) license (<https://creativecommons.org/licenses/by/4.0/>).

1. Introduction

Estuarine mud, commonly referred to as “cohesive sediment”, exhibits a unique tendency to flocculate in response to environmental changes, particularly variations in hydrodynamics, salinity, and organic matter abundance [1–5]. The floc populations which are formed play a crucial role in aquatic ecosystems, acting as dynamic reservoirs for contaminants and nutrients, thereby influencing water quality and biota distribution [6]. Consequently, accurately predicting the transport of flocculated particles is essential for effective environmental management and ecosystem protection.

Natural mud comprises sediment minerals and an organic matter fraction. Clay minerals such as kaolinite, illite, chlorite, smectite, and bentonite are the most common components of cohesive sediments [5]. The organic matter fraction consists of two main components: “dead” organic matter (including exopolymers produced by microorganisms) and “living” organic matter (microorganisms). Organic matter—in particular the

extra-cellular polymeric substances excreted by microorganisms [7–9]—significantly influences the cohesiveness, flocculation ability, deposition, consolidation, and erodibility of sediment [10–14].

Salinity also plays a crucial role in sediment flocculation. Flocculation is enhanced in saline environments [15], as observed at the transition between fresh and seawater in estuaries [16]. Flocs are significantly larger and settle at a faster rate than individual mineral particles, but they typically have a lower density [17,18]. The effective density of flocs decreases with increasing size [19–22]. In situ, flocs exhibit a wide range of structures, from individual clay particles to centimetre-long string-type flocs [13].

Additionally, flocs show a significant spread in settling velocity (and hence in density) for flocs in the range of 50–150 micrometres [13,21,23]. The settling velocity of solid, unaggregated silt and sand is straightforwardly determined by grain size using the Stokes settling velocity equation. However, the settling velocity of flocs is influenced by their size, effective density, shape, and porosity, all of which can rapidly change in response to local variations in the water column [24].

For long-term monitoring, continuous in situ laser-based diffraction techniques are employed, such as the Sequoia Scientific Laser In-situ Scattering and Transmissometry (LISST) 100× and 200×, which assess particle size and volume concentration [25]. These data can be used to estimate particle density and settling fluxes based on Stokes' law [26]. However, when flocs exhibit heterogeneous composition and non-spherical structures, LISST measurements should be interpreted with caution [13,27,28]. Additionally, in salinity-driven pycnoclines where the Schlieren effect distorts particle size measurements, LISSTs may provide unreliable data [29,30]. To address these limitations, supplementary monitoring campaigns are typically conducted episodically throughout the long-term measurement series. These campaigns involve sampling particles directly from the water column and characterising the properties of the suspended material using low-intrusive, high-resolution, video microscopy-based techniques [31–34].

These techniques involve carefully transferring a small quantity of the collected sample into a settling column using a proven modified pipetting technique (e.g., [35–37]). The particles are then recorded while settling, and their size, shape, and settling velocity are determined. The first objective of the research presented in this article is to study the dependency of the observed settling velocities on the concentration of particles by using two video microscopy devices. While neighboring particles can strongly affect a particle's settling velocity [19,38,39], it is still unclear if moderate changes in particle concentration significantly impact collective settling velocities. Another question is whether these changes can be detected using video microscopy. Finally, the results obtained from two different video microscopy setups and their associated softwares are analysed and compared.

In the present study, illite mineral clay is flocculated using an anionic polyacrylamide flocculant, and the settling velocities and sizes are determined using the two camera-based setups. The samples for a given clay differ only in particle concentration, but the flocculant to clay ratio is identical. Additional measurements are also made using a laboratory particle sizer (based on laser diffraction), similar to the LISST equipment used in situ.

The article is organised as follows: Section 2 provides an overview of the materials used and the experimental setups. Section 3 presents the relevant results and discussion. Finally, conclusions are given in Section 4.

2. Material and Methods

2.1. Clay

The experiments were performed using illite clay (100% illite) procured in dry powder form from Argiletz Laboratories. The median particle size (D_{50}) of the illite was determined

to be approximately 5 μm (see Supplementary Figure S1), measured using the Malvern Mastersizer 2000 (made by Malvern Panalytical, Malvern, Worcestershire, UK), which employs static light scattering for particle size analysis (Figure S2).

Four different clay concentrations (0.5, 1.0, 1.5, and 2.0 g L^{-1}) were used and flocculated by the addition of flocculant, keeping the ratio of flocculant concentration to clay concentration constant. All suspensions were flocculated in a jar for 1 h at a shear rate of 50 s^{-1} , which ensured that the flocculation reached a steady state.

2.2. Flocculant

Zetag 4110, an anionic polyacrylamide (produced by BTC Europe GmbH, Monheim am Rhein, Germany) with a medium anionic charge and a high molecular weight, was used as the flocculant in this study. A 2.5 mg g^{-1} flocculant to clay ratio was used for flocculation for all samples, which is close to the optimum dosage for this flocculant [40].

2.3. Water

All suspensions were prepared using tap water sourced from Evides, the local drinking water company. The composition of the tap water utilised during the experimental days is detailed in Table S1 of the Supplementary Material.

2.4. Floc Size and Settling Analysis

2.4.1. The LabSFLOC-2

The LabSFLOC-2 system (Figure 1), developed by Manning et al. [35,36,41–44], is based on a modified version of the in situ INSSEV instrument [45,46]. It utilises a high-magnification 2.0 MP Grasshopper monochrome digital video camera [42] to observe individual flocs as they settle within a 350 mm high by 100 mm square Perspex settling column. Positioned approximately 75 mm above the base of the column, the camera captures particles passing through a 1 mm depth of field in the centre of the column, 45 mm from a Sill TZM 1560 Telecentric lens. This lens, with 0.66 magnification (1:1.5), F4 aperture, and a maximum pixel distortion of 0.6%, is mounted behind a 5 mm-thick glass faceplate to ensure high-precision imaging. The LabSFLOC-2 can measure floc sizes (individual particles) nominally as small as 6 μm in diameter and settling velocities as high as 45 mm s^{-1} , allowing it to measure both pure mud and mud–sand mixed sediment floc dynamics. The floc porosity, fractal dimensions, floc dry mass, and mass settling flux of a floc population can be calculated by applying image analysis methods in MATLAB. During sampling, a modified pipette is used to carefully extract a sub-sample of the flocs. This sample is filled to create a fluid head of 50 mm in the pipette, resulting in a video control sample volume of approximately 400 mm^3 (with an image depth of 1 mm, a video image width of 8 mm, and a 50 mm-high suspension). This controlled volume allows the floc mass calculated by LabSFLOC-2 to be directly compared and calibrated against ambient suspended sediment concentrations (SSC) derived from filtered gravimetric analysis.

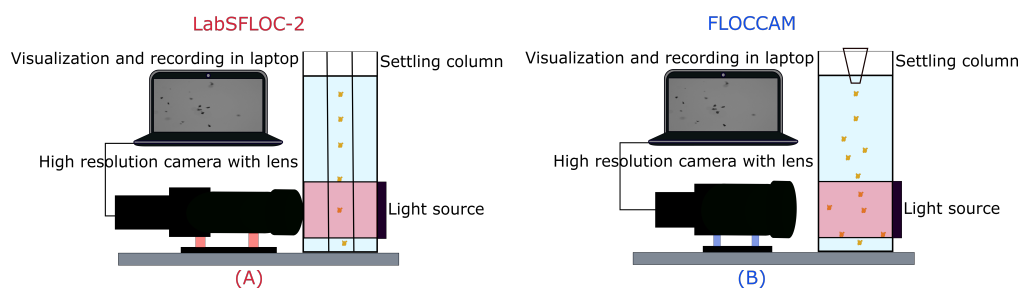


Figure 1. (A) Schematic representation of the LabSFLOC-2 setup [34] and (B) the FLOCCAM setup [47,48]. For physical pictures, see Figure S3.

Once extracted, the pipette sub-sample is immediately transferred to the LabSFLOC-2 settling chamber. The pipette's aperture is brought into contact with the water surface in the settling column, allowing the flocs to transfer naturally and settle under gravity without any external assistance. As the flocs settle, they become naturally segregated, with the fastest-settling aggregates being observed first due to differential settling. The settling flocs are visualised as silhouettes, reducing image smearing. This is achieved using a CCS LDL-TP-43/35-BL blue (470 nm) LED backlight panel, which provides homogeneous illumination from behind the settling column. The video footage is recorded in real-time as AVI files at a frame rate of 7.5 Hz (one frame every 0.04 s) with a resolution of 1600×1200 pixels, where each pixel corresponds to approximately $5 \mu\text{m}$, as confirmed by independent calibration. The AVI files remain uncompressed to allow for detailed analysis using MATLAB routines. In post-processing, the HR Wallingford Ltd DigiFloc software (version 1.0) [35,43] is used to semi-automatically analyze the video recordings, producing floc size distributions and settling velocity spectra.

2.4.2. FLOCCAM

The second video-based setup used is called FLOCCAM, which is inspired by LabSFLOC-2. The FLOCCAM device is designed to estimate particle size distributions (PSDs) larger than $20 \mu\text{m}$, as well as the settling velocities of floc samples [10,19,40,47,49–51]. Figure 1 provides a schematic overview of the equipment setup. The FLOCCAM setup is made of several parts. The rectangular settling column of dimensions $10 \text{ cm} \times 10 \text{ cm} \times 30 \text{ cm}$ has glass front and rear panels, while its sides are made of dark plastic. A 5 MP CMOS camera (model: iDS UI-3180CP-M-GL Rev.2.1, AB02546) with a resolution of 2592×2048 pixels and a pixel size of $4.8 \mu\text{m}$ is used to capture the settling process.

The camera is equipped with a Global Shutter for high-precision imaging. Paired with the camera is an S5VPJ2898 telecentric lens from Sill Optics GmbH and Co. KG, Wendelstein, Germany, featuring adjustable working distances and a C-mount, yielding an effective pixel size of approximately 8.6 mm. To ensure optimal lighting conditions during the experiments, a Flat Lights TH2 Series Red LED light panel (dimensions: $63 \text{ mm} \times 60 \text{ mm}$) is employed. This light source, renowned for its high directivity, is controlled by a CCS Inc. DC 24V Input Controller (model: PB-2430-1). Data recording and analysis are conducted using a Dell Inspiron-15-7590 laptop, which interfaces with the camera and software. Additionally, the experimental setup includes a conical plastic feed that is well designed to guide the flocs into the settling column. The feed well has a rectangular outlet measuring $2 \text{ mm} \times 10 \text{ mm}$. A pipette is used to carefully extract floc samples, which are then observed as they settle approximately 30 cm below the injection point, where their settling velocities are measured and recorded.

The PSD, shape, and settling velocity of the flocs are calculated from the recorded videos using a Python-based software package called Safas [47,52]. Safas, which stands for Sedimentation and Floc Analysis Software, is a specialised Python module developed for processing and analysing images and videos of flocs. This software enables users to directly extract and analyze key data from these images, providing measurements of size, morphology, and settling velocity in an intuitive, user-friendly format. As an open-source tool, Safas allows users to access and customise its image processing capabilities. The built-in filters, carefully designed and thoroughly tested, are optimised for segmenting and quantifying floc images. These filters employ a variety of functions to deliver precise, reliable analysis, making the software highly adaptable for both research and practical applications. The parameters described below were derived from video observations of the flocs:

2.4.3. Mean Diameter

Following the methodology adopted by several authors ([50,53]), the mean diameter (d_m) in micrometres (μm) was calculated as the geometric mean of the major axis diameter (d_{major}) and the minor axis diameter (d_{minor}) of the observed objects in the images:

$$d_m = \sqrt{(d_{major} \times d_{minor})} \tag{1}$$

Further discussions regarding the mean floc size (particularly in organic matter-rich flocs), floc structure, anisotropy, and uncertainties associated with 2D floc measurements can be found in ([13,54]).

2.4.4. Aspect Ratio

The aspect ratio (AR) of the flocs was determined using their major axis diameter (d_{major}) and minor axis diameter (d_{minor}) through the following relationship:

$$AR = \frac{d_{major}}{d_{minor}} \tag{2}$$

2.4.5. Effective Floc Density

The effective floc density (ρ_f) was estimated under the assumption of Stokes' law validity:

$$\rho_f = \rho_w + \frac{9\eta v}{2gR_f^2} \tag{3}$$

Here, ρ_w denotes the density of water, η represents the dynamic viscosity of water, v is the settling velocity of the floc, g stands for gravitational acceleration, and R_f corresponds to the floc radius. The mean floc density was determined by averaging density values across different floc sizes.

2.4.6. Fractal Dimension

When considering flocs as fractal entities composed of primary particles of size a , the volume fraction of solids (ϕ_s) within a floc is expressed as follows:

$$\phi_s = \frac{N \cdot a^3}{R_f^3} = \left(\frac{R_f}{a}\right)^{D-3} \tag{4}$$

where N is the number of solid particles in a floc, and D represents the fractal dimension. The density of the flocs can be related to the solid volume fraction through the following:

$$\frac{(\rho_f - \rho_w)}{\rho_s} = \frac{\phi_s(\rho_s - \rho_w)}{\rho_s} \tag{5}$$

Combining the solid (clay) density (ρ_s) with Equations (4) and (5), the resulting expression becomes the following:

$$(\rho_f - \rho_w) = (\rho_s - \rho_w) \left(\frac{R_f}{a}\right)^{D-3} \tag{6}$$

The fractal dimension D can be derived by fitting $\rho_f - \rho_w$ as a function of R_f , as demonstrated by [55,56]. However, natural flocs are not true fractals. Therefore, the term "pseudo-fractal dimension", as suggested by [1,7], is more appropriate.

3. Results and Discussion

Figure 2 illustrates the particle size distribution (PSD) of flocs as measured by the Malvern Mastersizer for the different clay concentrations. As shown in Figure 2A, the median floc size is as large as 1 mm for the highest clay concentrations. For 0.5 g L^{-1} , the median floc size is about 300 microns. This is due to the slow flocculation kinetics at this low clay concentration. It was observed, for the shear rate used during the one-hour flocculation, that particles settled at the bottom of the jar (which was not observed for the other concentrations), similarly to what was observed in Ali et al. [19]. Figure 2B,C present the PSD based on volume and number percentages, respectively. The peaks observed for the 1.5 g L^{-1} concentration in Figure 2C differ from those of other concentrations due to the absence of particles within the 0.01–100 micron size range at this concentration. The comparison between volume-based and particle-based statistics illustrates well the challenges faced when comparing the results of laser diffraction methods (such as the Malvern particle sizer in the lab or the LISST in situ), which rely on volume-based averages and video microscopy methods (such as LabsFLOC-2 or FLOCCAM), which in turn rely on number-based averages. Even though laser diffraction enables to assess particles as small as 10 nm, it is often observed, as illustrated here, when the data for 1.5 g L^{-1} are compared with the data for 1 or 2 g L^{-1} , that the large particles “overshadow” the smaller ones. The largest particles peak in this case with a size close to 1 mm, which might also not be representative for the correct particle size distribution of the large-size particles, as the size peak is “smoothened” by the software [57].

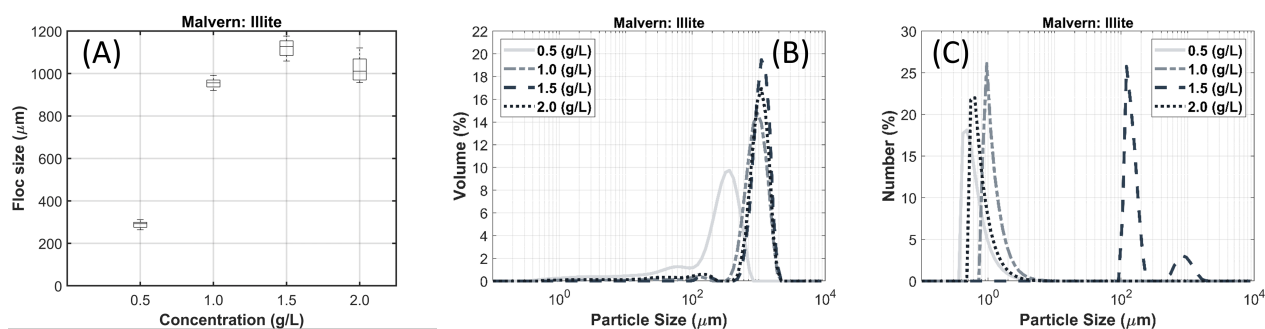


Figure 2. Flocculated illite clay at different clay concentration. (A) Median floc size obtained with Malvern ParticleSizer. (B) Volume-based particle size distribution obtained from the ParticleSizer. (C) Number-based particle size distribution recalculated from the data displayed in (B).

Figure 3 presents the particle size and settling velocity results for flocculated illite at a concentration of 0.5 g L^{-1} , measured using FLOCCAM and LabSFLOC-2. In Figure 3A,D, the FLOCCAM videos were processed with the Safas software package, while LabSFLOC-2 videos were analyzed using an image analysis tool in MATLAB. The results indicate that the floc sizes and settling velocities are consistent between the two methods. However, a difference in the number of flocs measured by each setup is noted, as it is clear that more smaller flocs are recorded using the FLOCCAM. Figure 3B,E display the particle sizes and settling velocities found from the FLOCCAM video data analyzed using both Safas and MATLAB. The comparison between the results is in good agreement, even though the number of smallest particles detected is higher using the Safas software. In Figure 3C,F, the LabSFLOC-2 video is analysed using both Safas and MATLAB. The number of flocs detected is low when using both softwares. The differences in the number of flocs recorded using either FLOCCAM or LabsFLOC-2 is mainly due to the quality of the videos. The camera system of FLOCCAM is of better quality than the one of LabsFLOC-2 (which is of an older generation). It is, however, not excluded that some differences also come from variations in the number of flocs pipetted for each video recording. We emphasise that the full lengths of the videos were analyzed for all samples analysed (i.e., every settling floc present in each sample was measured).

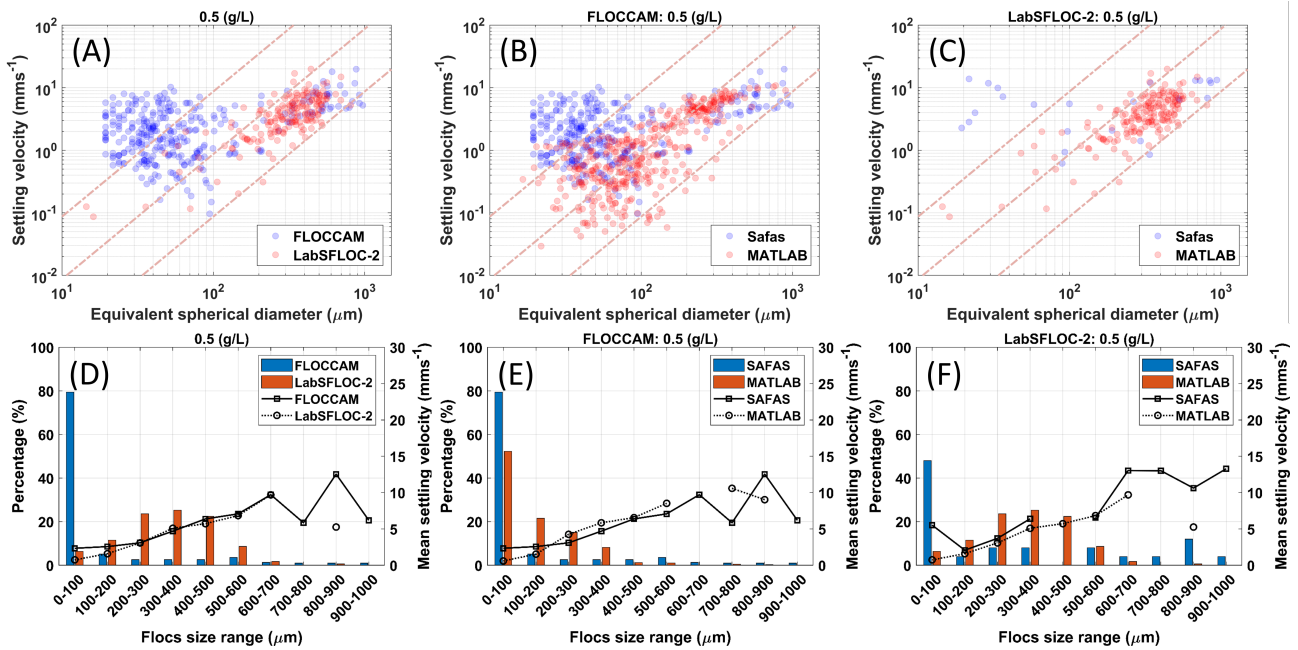


Figure 3. Comparison of floc sizes and settling velocities for flocculated illite clay at 0.5 g L^{-1} clay concentration using different setups (LabsFLOC-2 and FLOCCAM) and software (Matlab and Safas). Panels (A,D): videos obtained from LabsFLOC-2 and FLOCCAM and analysed with their respective softwares (Matlab, Safas). Panels (B,E): video obtained from FLOCCAM analysed using the two softwares. Panels (C,F): video obtained from LabsFLOC-2 analysed using the two softwares. Upper panels: diagonal dashed lines representing effective density iso-lines calculated by using Stokes equation (from left to right: 1600, 160, 16 (kg m^{-3})). Bottom panels: bars indicate sizes and black curves indicate settling velocities.

The software analysis comparison shows that the flocs detected do not completely match: with the Safas software, more small particles are detected. This results in a mismatch in bin sizes for the [0–100] micron-size particles. The recorded settling velocities are overall in excellent agreement. The mean settling velocity for the [0–100] micron-size particles is higher when evaluated by Safas, confirming that the Safas video can be used to track small mineral-rich (unflocculated or poorly flocculated) particles (usually of size close to 20 microns—i.e., the threshold of the software). A large amount of small particles were also found using the Malvern particle sizer (see Figure 2C). On the other hand, it appears that the MATLAB software can better track the large particles (see Figure 3C,F). Flocs of large sizes have a large amount of organic matter, which is optically (semi-)transparent and makes it complicated for the software to detect flocs containing large amounts of organic matter.

The results for 2.0 g L^{-1} concentration are shown in Figure 4. The results are consistent with 0.5 g L^{-1} ; however, there is an overall slight increase in floc size and settling velocities compared to the 0.5 g L^{-1} case. The observations at 0.5 g L^{-1} (see Figure 3B,C,E,F) indicate that the MATLAB software is more effective in tracking larger particles, while the Safas software excels at tracking smaller particles. The settling velocity (as was the case of the 0.5 g L^{-1} case) displays a slight increasing trend as function of increasing size, but it is clear that the settling velocity cannot be approximated by a Stokes equation (which is a function of the square of the particle size). Note that, as for the 0.5 g L^{-1} , flocs of a larger size (above 300 microns) roughly follow an iso-density line with a density in the range $[16\text{--}160] \text{ kg m}^{-3}$, corresponding to flocculant-rich particles. This would tend to suggest that the largest flocs have a constant density and that therefore these flocs always encapsulate the same amount of flocculant and clay particles. Small flocs, on the other hand, have a large spread in settling velocities and

follow no trend. The fact that flocs of very different sizes have the same settling velocity is likely due to the collective effects as discussed in [10].

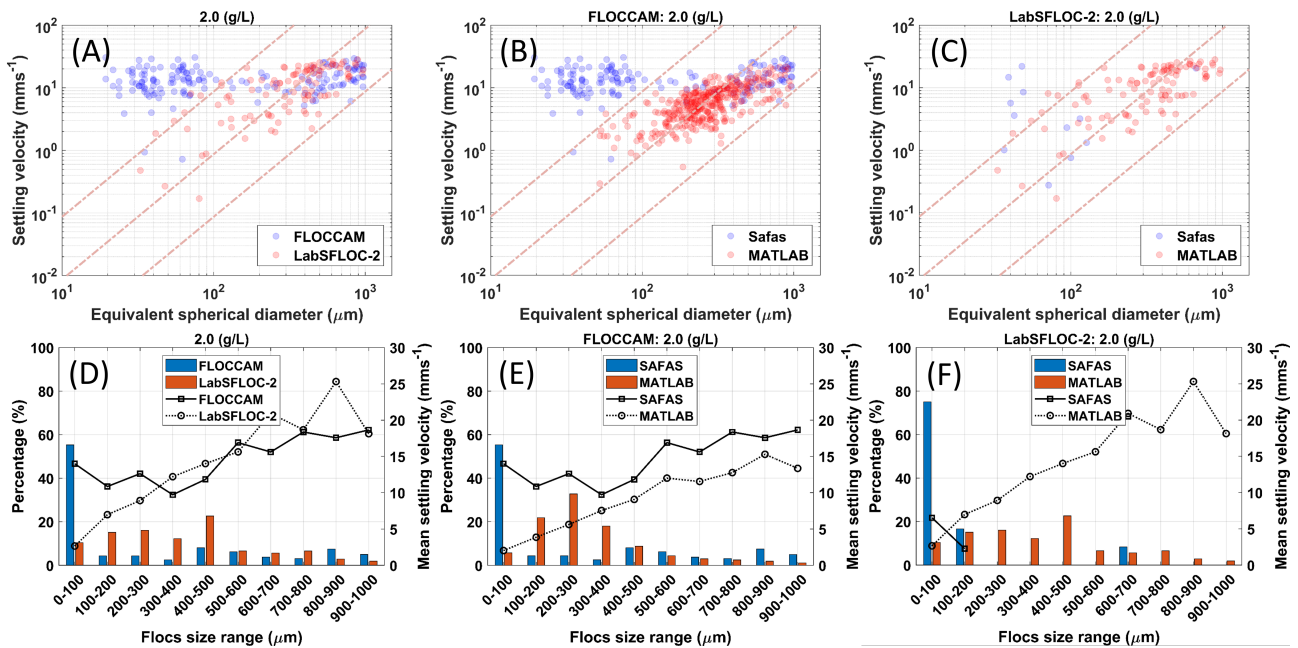


Figure 4. Comparison of floc sizes and settling velocities for flocculated illite clay at 2.0 g L^{-1} clay concentration using different setups (LabsFLOC-2 and FLOCCAM) and software (Matlab and Safas). Panels (A,D): videos obtained from LabsFLOC-2 and FLOCCAM and analysed with their respective softwares (Matlab, Safas). Panels (B,E): video obtained from FLOCCAM analysed using the two softwares. Panels (C,F): video obtained from LabsFLOC-2 analysed using the two softwares. Upper panels: diagonal dashed lines representing effective density iso-lines calculated by using Stokes equation (from left to right: 1600, 160, 16 (kg m^{-3})). Bottom panels: bars indicate sizes and black curves indicate settling velocities.

The results for other concentrations are provided in Supplementary Figures S3 and S4. The data obtained for all concentrations are summarised in Figure 5. In that figure, floc sizes and settling velocities are obtained using the two different setups and the different softwares. The assessment revealed, in line with the observations made above, that the Safas software can track the smaller particles more efficiently, and the MATLAB-based approach was more effective for the larger floc size fractions. The largest number of particles is found for sizes below 100 microns for the FLOCCAM setup, whereas the largest amount of particles is observed at around 300 microns for the LabsFLOC-2 setup (the particles of this size are seen as outliers in Safas). Both setups show an increase in average settling velocity as a function of increasing clay concentration, whereas floc sizes do not vary much over the range of concentrations. All floc samples were created in the same way, as detailed in Section 2. In particular, the illite clay and flocculant was mixed in all cases for one hour, allowing floc sizes to reach a steady-state. Over time, as already studied in [58,59], flocs tend to become denser as the strands of organic matter coil onto the clay platelets. At 2.0 g L^{-1} , the flocculation kinetics are the fastest and therefore flocs formed at 2.0 g L^{-1} clay can become denser than flocs formed at a lower clay concentration. This implies that, for the same sizes, particles settle faster. For flocs of smaller sizes (in the range [0–100] microns), it was already noted that collective settling may be present. The mean settling velocity, for example, of 20 micron flocs made of clay material, should be in the range of 0.5 mm s^{-1} , according to the Stokes equation. From the data for all concentrations, it can be seen that many flocs of this size settle as fast as 10 mm s^{-1} , which does not correspond to any realistic density. The observed collective settling could also be partially attributed to the duration that the pipette is held in contact

with the settling column fluid and thus the nominal number of flocs released into the clear water of the column, relative to the ambient SSC from the suspension where the flocs were originally created and extracted from.

It is also observed that the mean settling velocity of flocs in the [0–100] microns size range increases with concentration when the FLOCCAM videos are analysed with Safas. The average settling velocities are found to be 2.3, 3.7, 4.6, and 14 mm s⁻¹ for 0.5, 1, 1.5, and 2.0 g L⁻¹, respectively. One could argue that this increase in settling velocity is due to the increase in density difference between the water (devoid of flocs) and the portion of fluid containing the flocs. However, as explained above, it was also found that the settling velocities of large flocs increases with concentration, and this is certainly also a factor to account for.

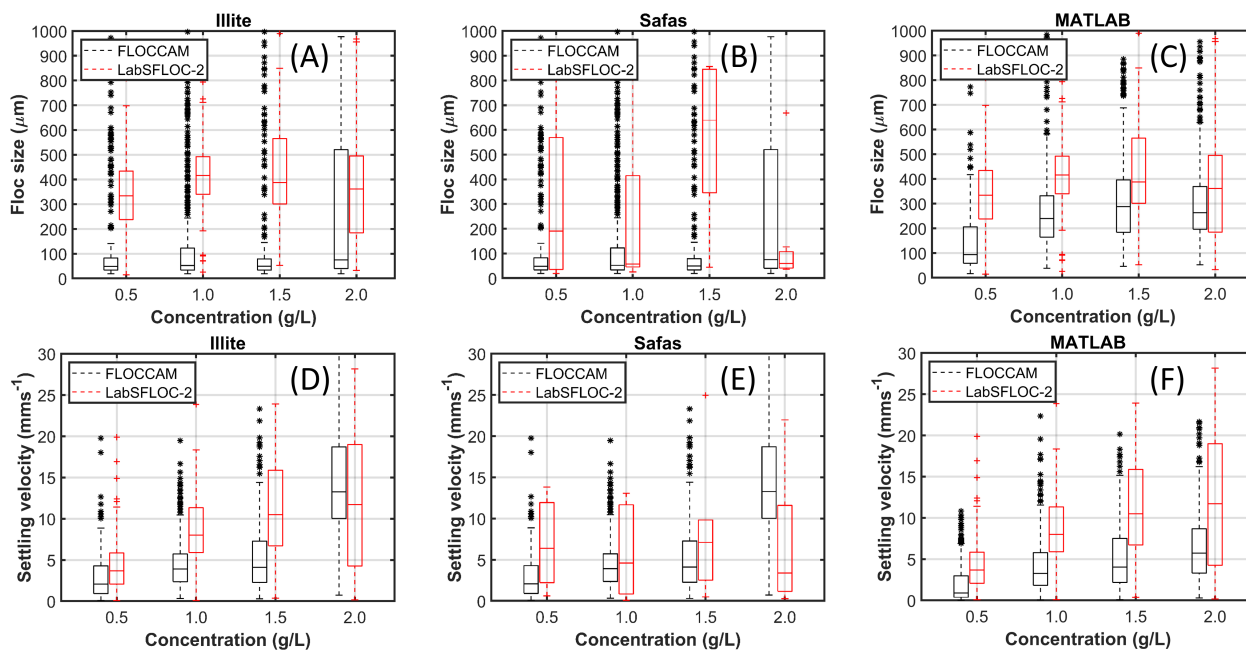


Figure 5. Comparison of floc sizes and settling velocities for different concentrations. Panels (A,D): videos obtained from LabsFLOC-2 and FLOCCAM and analysed with their respective softwares (Matlab, Safas). Panels (B,E): video obtained from FLOCCAM analysed using the two softwares. Panels (C,F): video obtained from LabsFLOC-2 analysed using the two softwares.

4. Conclusions

In this work, we compare two video microscopy setups, LabSFLOC-2 and FLOCCAM, and study floc sizes and settling velocities for four different samples made with different illite clay concentrations but the same flocculant to clay ratio. The flocs size and settling velocities obtained with the help of LabSFLOC-2 and FLOCCAM compare quite well with each other. Overall, it is found that LabsFLOC-2 can better track the larger particles (because its related software can better accommodate the low-contrast organic matter-rich flocs), and FLOCCAM can better track the smallest ones (because the lens and camera are of better quality). By studying the two floc analysis softwares more in-depth in the future, we hope to improve the floc tracking of Safas.

In this study, we also wanted to verify whether reasonable changes in particle concentration would influence the collective settling of flocs. It was found that this question could not be well answered due to the dynamic nature of flocs and the large spread in both settling velocity and size. However, we postulate that aspects of the collective settling effect could be partly attributed to being a function of the duration that the flocs are initially released and introduced into the settling column from the modified pipette for different SSCs, and slight adjustments in this procedure could reduce collective settling. It was found that the settling

velocity of flocs increased with clay concentration, but that the average size of flocs barely increased. Even though all the samples were created using the same protocol, the reason was attributed to the difference in the coiling of the organic matter that composes the flocs. This coiling is faster when the clay concentration is higher (as the collision frequency is then higher), and this implies that after one hour of flocculation, the flocs created with 2.0 g L^{-1} clay concentration were denser than the flocs created with 0.5 g L^{-1} of clay. For this reason, flocs would settle faster at high clay concentrations. At the same time, the density difference between water (devoid of flocs) and the portion of fluid containing flocs that is analysed is increasing with clay concentration. This would also lead to an increase in settling velocity. At this stage, it is not possible to conclude which factor is predominant, and the experiments should be repeated with flocs of the same size and densities, at different floc concentrations.

Using an image-based device to observe suspended sediment characteristics provides a unique opportunity to visualise and characterise the particles that comprise a certain particle population. When compared to non-optical particle sizing instruments, particle sizing with an image-based device like the LabSFLOC-2 and FLOCCAM provides useful information required for the characterisation of cohesive sediment. Therefore, it is possible to determine floc population characteristics directly without the need for extra observations or assumptions that would be required for laser diffraction-based particle sizing devices.

Supplementary Materials: The following supporting information can be downloaded at <https://www.mdpi.com/article/10.3390/jmse13020212/s1>: Figure S1: Particle size distribution of an unflocculated illite suspension, measured using the set-up described in S2; Figure S2: Schematic of Malvern Master Sizer 2000 setup; Figure S3: (Top) Picture of LabSFLOC-2 (Bottom) Picture of FLOCCAM; Figure S4: Comparison of floc size and settling velocities for 1 g/L illite clay suspension flocculated using 2.5 mg/g anionic polyacrylamide; Figure S4: Comparison of floc size and settling velocities for 1.5 g/L illite clay suspension flocculated using 2.5 mg/g anionic polyacrylamide; Table S1: Tap water specifications.

Author Contributions: W.A. first draft manuscript and sample preparation. W.A. and A.J.M. floc settling experiments and analysis. A.K., A.J.M., and C.C. contributed to data analysis and interpretation. All authors have read and agreed to the published version of the manuscript.

Funding: This work is performed in the framework of PlumeFloc (TMW.BL.019.004, Topsector Water and Maritiem: Blauwe route) within the MUDNET academic network. AJM's contribution towards this research was also partly supported by the US National Science Foundation under grants OCE-1736668 and OCE-1924532, TKI-MUSA Project 11204950-000-ZKS-0002, and HR Wallingford Company Research projects: 'FineScale' (ACK3013 62) and 'Support for QMUL Floc Research' (DDY0524).

Institutional Review Board Statement: Not applicable for this study as it did not involve humans or animals.

Informed Consent Statement: Not applicable for this study as it did not involve humans or animals.

Data Availability Statement: The data used in this study is included in the article itself and in the Supplementary Material. Further inquiries can be directed to the corresponding author.

Acknowledgments: The authors would like to thank all co-funding partners. The authors would also like to thank Deltares for using their experimental facilities in the framework of the MoU between TU Delft/Deltares.

Conflicts of Interest: The authors declare no conflict of interest.

References

1. Chassagne, C. *Introduction to Colloid Science*; Delft Academic Press: Delft, The Netherlands, 2020; ISBN 9789065624376.
2. Guo, C.; Jin, Z.; Zhou, Y. Investigation of Flocculation Characteristics in the Yangtze Estuary. In *Estuary Research—Recent Advances*; InTech Open: Rijeka, Croatia, 2023.

3. Manning, A.J. Observations of the properties of flocculated cohesive sediment in three western European estuaries. *J. Coast. Res.* **2004**, *41*, 70–81.
4. Mehta, A.J. An Introduction to Hydraulics of Fine Sediment Transport. In *Advanced Series on Ocean Engineering*; World Scientific Publishing Co.: Hackensack, NJ, USA, 2014; Volume 38.
5. Whitehouse, R.J.S.; Soulsby, R.; Roberts, W.; Mitchener, H.J. *Dynamics of Estuarine Muds*; Thomas Telford Publications: London, UK, 2000.
6. Uncles, R.J.; Stephens, J.A.; Harris, C. Seasonal variability of subtidal and intertidal sediment distributions in a muddy, macrotidal estuary: The Humber-Ouse, UK. In *Sedimentary Processes in the Intertidal Zone*; Black, K.S., Paterson, D.M., Cramp, A., Eds.; Geological Society Special Publications: London, UK, 1998; Volume 139, pp. 211–219.
7. Malarkey, J.; Baas, J.H.; Hope, J.A.; Aspden, R.J.; Parsons, D.R.; Peakall, J.; Paterson, D.M.; Schindler, R.J.; Ye, L.; Lichtman, I.D.; et al. The pervasive role of biological cohesion in bedform development. *Nat. Commun.* **2015**, *6*, 6257. [[CrossRef](#)] [[PubMed](#)]
8. Parsons, D.R.; Schindler, R.J.; Hope, J.A.; Malarkey, J.; Baas, J.H.; Peakall, J.; Manning, A.J.; Ye, L.; Simmons, S.; Paterson, D.M.; et al. The role of biophysical cohesion on subaqueous bed form size. *Geophys. Res. Lett.* **2016**, *43*, 1566–1573. [[CrossRef](#)] [[PubMed](#)]
9. Tolhurst, T.J.; Gust, G.; Paterson, D.M. The influence on an extra-cellular polymeric substance (EPS) on cohesive sediment stability. In *Fine Sediment Dynamics in the Marine Environment—Proceedings in Marine Science 5*; Winterwerp, J.C., Kranenburg, C., Eds.; Elsevier: Amsterdam, The Netherlands, 2002; pp. 409–425. ISBN 0-444-51136-9.
10. Ali, W. Flocculation and Deep-Sea Mining Plumes. Ph.D. Thesis, Delft University of Technology, Delft, The Netherlands, 2024.
11. Heinzlmann, C.H.; Wallisch, S. Benthic settlement and bed erosion. A review. *J. Hydraul. Res.* **1991**, *29*, 355–371. [[CrossRef](#)]
12. Nowell, A.R.M.; Jumars, P.A.; Eckman, J.E. Effects of biological activities on the entrainment of marine sediments. *Mar. Geol.* **1981**, *42*, 133–153. [[CrossRef](#)]
13. Safar, Z. Suspended Particulate Matter Formation and Accumulation in the Delta: From Monitoring to Modelling. Ph.D. Thesis, Delft University of Technology, Delft, The Netherlands, 2022.
14. Shakeel, A.; Ali, W.; Kirichek, A.; Chassagne, C. Tuning the rheological properties of kaolin suspensions using biopolymers. *Colloids Surfaces A Physicochem. Eng. Asp.* **2022**, *654*, 130120. [[CrossRef](#)]
15. Krahl, E.; Vowinkel, B.; Ye, L.; Hsu, T.-J.; Manning, A.J. Impact of the Salt Concentration and Biophysical Cohesion on the Settling Behavior of Bentonites. *Front. Earth Sci. (Mar. Geosci.)* **2022**, *10*, 886006. [[CrossRef](#)]
16. Van Leussen, W. The variability of settling velocities of suspended fine-grained sediment in the ems estuary. *J. Sea Res.* **1999**, *41*, 109–118. [[CrossRef](#)]
17. Dyer, K.R.; Manning, A.J. Observation of the size, settling velocity and effective density of flocs, and their fractal dimensions. *J. Sea Res.* **1999**, *41*, 87–95. [[CrossRef](#)]
18. McDowell, D.N.; O'Connor, B.A. *Hydraulic Behaviour of Estuaries*; MacMillan: London, UK, 1977.
19. Ali, W.; Kirichek, A.; Chassagne, C. Collective effects on the settling of clay flocs. *Appl. Clay Sci.* **2024**, *254*, 107399. [[CrossRef](#)]
20. Droppo, I.G.; Walling, D.; Ongley, E. The influence of floc size, density and porosity on sediment and contaminant transport. *J. Natl. Cent. Sci. Res.* **2000**, *4*, 141–147.
21. Khelifa, A.; Hill, P.S. Models for effective density and settling velocity of flocs. *J. Hydraul. Res.* **2006**, *44*, 390–401. [[CrossRef](#)]
22. Klimpel, R.C.; Hogg, R. Effects of flocculation conditions on agglomerate structure. *J. Colloid Interface Sci.* **1986**, *113*, 121–131. [[CrossRef](#)]
23. Maggi, F. The settling velocity of mineral, biomineral, and biological particles and aggregates in water. *J. Geophys. Res. Ocean.* **2013**, *118*, 2118–2132. [[CrossRef](#)]
24. Manning, A.J. The observed effects of turbulence on estuarine flocculation. *J. Coast. Res.* **2004**, *41*, 90–104.
25. Agrawal, Y.C.; Pottsmith, H.C. Instruments for particle size and settling velocity observations in sediment transport. *Mar. Geol.* **2000**, *168*, 89–114. [[CrossRef](#)]
26. Fettweis, M. Uncertainty of excess density and settling velocity of mud flocs derived from in situ measurements. *Estuarine Coast. Shelf Sci.* **2008**, *78*, 426–436. [[CrossRef](#)]
27. Mikkelsen, O.A.; Hill, P.S.; Milligan, T.G.; Chant, R.J. In situ particle size distributions and volume concentrations from a LISST-100 laser particle sizer and a digital floc camera. *Cont. Shelf Res.* **2005**, *25*, 1959–1978. [[CrossRef](#)]
28. Smith, S.J.; Friedrichs, C.T. Size and settling velocities of cohesive flocs and suspended sediment aggregates in a trailing suction hopper dredge plume. *Cont. Shelf Res.* **2011**, *31*, S50–S63. [[CrossRef](#)]
29. Chapalain, M.; Verney, R.; Fettweis, M.; Jacquet, M.; Le Berre, D.; Le Hir, P. Investigating suspended particulate matter in coastal waters using the fractal theory. *Ocean. Dyn.* **2019**, *69*, 59–81. [[CrossRef](#)]
30. Karageorgis, A.; Georgopoulos, D.; Gardner, W.; Mikkelsen, O.; Velaoras, D. How schlieren affects beam transmissometers and LISST-Deep: An example from the stratified Danube River delta, NW Black Sea. *Mediterr. Mar. Sci.* **2015**, *16*, 366–372. [[CrossRef](#)]
31. Fall, K.A.; Friedrichs, C.T.; Massey, G.M.; Bowers, D.G.; Smith, S.J. The importance of organic content to fractal floc properties in estuarine surface waters: Insights from video, LISST, and pump sampling. *J. Geophys. Res. Ocean.* **2021**, *126*, 1–25. [[CrossRef](#)]

32. Law, D.J.; Bale, A.J.; Jones, S.E. Adaptation of focused beam reflectance measurement to in-situ particle sizing in estuaries and coastal waters. *Mar. Geol.* **1997**, *140*, 47–59. [[CrossRef](#)]
33. Manning, A.J.; Baugh, J.V.; Soulsby, R.L.; Spearman, J.R.; Whitehouse, R.J.S. Cohesive sediment flocculation and the application to settling flux modelling. In *Sediment Transport*; Ginsberg, S.S., Ed.; InTech: Rijeka, Croatia, 2011.
34. Manning, A.J. *LabSFLOC-2—The Second Generation of the Laboratory System to Determine Spectral Characteristics of Flocculating Cohesive and Mixed Sediments*; HR Wallingford Report; HR Wallingford: Wallingford, UK, 2015.
35. Manning, A.J.; Whitehouse, R.J.S.; Uncles, R.J. Suspended particulate matter: The measurements of flocs. In *ECSA Practical Handbooks on Survey and Analysis Methods: Estuarine and Coastal Hydrography and Sedimentology*; Cambridge University Press: Cambridge, UK, 2017; pp. 211–260.
36. Ye, L.; Manning, A.J.; Hsu, T.-J.; Morey, S.; Chassignet, E.P.; Ippolito, T.A. Novel Application of Laboratory Instrumentation Characterizes Mass Settling Dynamics of Oil-Mineral Aggregates (OMAs) and Oil-Mineral-Microbial Interactions. *Mar. Technol. Soc. J. Technol. Cent. Overv.* **2018**, *52*, 87–90. [[CrossRef](#)]
37. Abolfazli, E.; Strom, K. Salinity impacts on floc size and growth rate with and without natural organic matter. *J. Geophys. Res. Ocean.* **2023**, *128*, e2022JC019255. [[CrossRef](#)]
38. Ali, W.; Kirichek, A.; Chassagne, C. Flocculation of deep-sea clay from the Clarion Clipperton fracture zone. *Appl. Ocean. Res.* **2024**, *150*, 104099. [[CrossRef](#)]
39. Gomez, D.C.; Bergougnoux, L.; Guazzelli, E.; Hinch, E.J. Fluctuations and stratification in sedimentation of dilute suspensions of spheres. *Phys. Fluids* **2009**, *21*, 093304. [[CrossRef](#)]
40. Shakeel, A.; MacIver, M.R.; van Kan, P.J.M.; Kirichek, A.; Chassagne, C. A rheological and microstructural study of two-step yielding in mud samples from a port area. *Colloids Surfaces A Physicochem. Eng. Asp.* **2021**, *624*, 126827. [[CrossRef](#)]
41. Manning, A.J. *LabSFLOC—A Laboratory System to Determine the Spectral Characteristics of Flocculating Cohesive Sediments*; Wallingford Technical Report TR 156; HR Wallingford: Wallingford, UK, 2006; Volume 26.
42. Manning, A.J.; Dyer, K.R. A Comparison Of Floc Properties Observed During Neap and Spring Tidal. *Proc. Mar. Sci.* **2002**, *5*, 233–250.
43. Benson, T.; Manning, A. *Digifloc: The Development of Semi-Automatic Software to Determine the Size and Settling Velocity of Flocs*; HR Wallingford: Wallingford, UK, 2016.
44. Ye, L.; Penaloza-Giraldo, J.A.; Manning, A.J.; Holyoke, J.; Hsu, T.J. Biophysical flocculation reduces variability of cohesive sediment settling velocity. *Commun. Earth Environ.* **2023**, *4*, 138. [[CrossRef](#)]
45. Manning, A.J.; Dyer, K.R. The use of optics for the in situ determination of flocculated mud characteristics. *J. Opt. Pure Appl. Opt.* **2002**, *4*, S71. [[CrossRef](#)]
46. Fennessy, M.J.; Dyer, K.R.; Huntley, D.A. INSSEV: An instrument to measure the size and settling velocity of flocs in-situ. *Mar. Geol.* **1994**, *117*, 107–117. [[CrossRef](#)]
47. Ali, W.; Enthoven, D.; Kirichek, A.; Helmons, R.; Chassagne, C. Effect of flocculation on turbidity currents. *Front. Earth Sci.* **2022**, *10*, 1014170. [[CrossRef](#)]
48. Ali, W.; Enthoven, D.; Kirichek, A.; Helmons, R.; Chassagne, C. Can flocculation reduce the dispersion of deep sea sediment plumes? In Proceedings of the World Dredging Conference, Copenhagen, Denmark, 16–20 May 2022.
49. de Lange, S.I.; van der Wilk, A.; Chassagne, C.; Ali, W.; Born, M.P.; Brodersen, K.; Waldschläger, K. Migrating subaqueous dunes capture clay flocs. *Commun. Earth Environ.* **2024**, *5*, 729. [[CrossRef](#)]
50. Manning, A.; Friend, P.; Prowse, N.; Amos, C. Estuarine mud flocculation properties determined using an annular mini-flume and the LabSFLOC system. *Cont. Shelf Res.* **2007**, *27*, 1080–1095. [[CrossRef](#)]
51. Wahab, S.A.; Ali, W.; Chassagne, C.; Helmons, R. Role of Organic Matter Present in the Water Column on Turbidity Flows. *J. Mar. Sci. Eng.* **2024**, *12*, 1884. [[CrossRef](#)]
52. MacIver, M.R. Safas: Sedimentation and Floc Analysis Software. 2019. Available online: <https://github.com/rmaciver/safas> (accessed on 1 January 2020).
53. Ye, L.; Manning, A.J.; Hsu, T.-J. Corrigendum to “oil-mineral flocculation and settling velocity in saline water”. *Water Res.* **2020**, *173*, 115569. [[CrossRef](#)]
54. Spencer, K.; Wheatl, J.; Carr, S.; Manning, A.; Bushby, A.; Gu, C.; Botto, L.; Lawrence, T. Quantification of 3 dimensional structure and properties of flocculated natural suspended sediment. *Water Res.* **2022**, *222*, 118835. [[CrossRef](#)]
55. Guo, C.; Manning, A.J.; Bass, S.; Guo, L.; He, Q. A quantitative lab examination of floc fractal property considering influences of turbulence, salinity and sediment concentration. *J. Hydrol.* **2021**, *601*, 126574. [[CrossRef](#)]
56. Manning, A.J.; Dyer, K. A laboratory examination of floc characteristics with regard to turbulent shearing. *Mar. Geol.* **1999**, *160*, 147–170. [[CrossRef](#)]
57. Ibanez Sanz, M. Flocculation and Consolidation of Cohesive Sediments Under the Influence of Coagulant and Flocculant. Ph.D. Thesis, Delft University of Technology, Delft, The Netherlands, 2018. [[CrossRef](#)]

-
58. Ali, W.; Chassagne, C. Comparison between two analytical models to study the flocculation of mineral clay by polyelectrolytes. *Cont. Shelf Res.* **2022**, *250*, 104864. [[CrossRef](#)]
 59. Shakeel, A.; Safar, Z.; Ibanez, M.; Paassen, L.; Chassagne, C. Flocculation of clay suspensions by anionic and cationic polyelectrolytes a systematic analysis. *Minerals* **2020**, *10*, 999. [[CrossRef](#)]

Disclaimer/Publisher's Note: The statements, opinions and data contained in all publications are solely those of the individual author(s) and contributor(s) and not of MDPI and/or the editor(s). MDPI and/or the editor(s) disclaim responsibility for any injury to people or property resulting from any ideas, methods, instructions or products referred to in the content.